Nuclear Structure Effects in High-Energy (p,pn) Reactions*

NORBERT T. PORILE AND SHIGEO TANAKA
Chemistry Department, Brookhaven National Laboratory, Upton, New York
(Received 9 January 1963)

Cross sections for the (p,pn) reaction of Cu^{65}, Zn^{66}, Ge^{70}, Ge^{72}, Se^{76}, Br^{79}, and Br^{81} have been measured at 2.9 GeV. The following variation with target neutron number is indicated by these results, as well as by recent measurements for Ga^{69}, Ga^{71}, and As^{75}: The (p,pn) cross sections increase from 50 mb at $N=36$ to 64 mb at $N=40$, then decrease to 48 mb at $N=42$, and finally increase to 59 mb at $N=46$. The results are compared with Benioff's calculation of (p,pn) cross sections and good agreement is obtained on the assumption that the $1f_{7/2}$ shell is available for the (p,pn) reaction up to $N=40$ and unavailable thereafter. The effect of nuclear deformation on the availability of this shell is considered in detail and is found to be small.

I. INTRODUCTION

THE application of experiments involving high bombarding energies to nuclear structure studies has received increasing attention in recent years. The interest in these experiments is related to the fact that distortion effects due to initial- and final-state interactions decrease at high energies so that it is more readily possible to obtain information about the nuclear wave functions. The $(p,2$ nucleon) reaction has received the greatest attention in this connection because at high energies it primarily involves the knock-out of a target nucleon by the incident proton, while the rest of the nucleus remains undisturbed. The energy spectrum of the outgoing nucleons, therefore, reflects the energy distribution of nucleons within the target nucleus and this yields information that may be compared with various nuclear models. The summed energy spectrum of protons emitted in high-energy $(p,2p)$ reactions in light elements has been investigated by Tyrén, Hillman, and Maris,[1,2] and more recently by several other groups.[3] These experiments give information on the binding energy of different proton shells and on their energy broadening. Gamma-ray emission in the de-excitation of bound excited states formed as the result of $(p,2$ nucleon) reactions at high energies has been investigated by Foley, Salmon, and Clegg.[4,5] These experiments give information on the parentage of the target ground state.

The relation between cross sections for high-energy (p,pn) reactions and nuclear structure has recently been considered by Benioff.[6] He has shown that (p,pn) cross sections are related to the number of neutrons in all nuclear shells for which the removal of a neutron leaves the nucleus in an excited "hole" state stable to particle emission. It may, therefore, be possible to obtain information about the number of nuclear shells fullfilling this condition from the magnitude of a given (p,pn) reaction cross section. Further, as nuclear shells become filled they move to lower energies in the potential well of the nucleus and at some point become unavailable for the (p,pn) reaction. If the number of neutrons in such a shell constitutes a substantial fraction of the total number of available neutrons it may be possible to observe a corresponding decrease in the (p,pn) cross section. It was thus suggested by Grover[7] on the basis of considerations similar to those outlined above that such an effect might occur in the region of the gallium isotopes due to the sudden unavailability of the $1f_{7/2}$ shell. The occurrence of such an effect can thus give information on the energy difference between a given shell and the topmost shell and would also constitute confirmatory evidence for the proposed[6] mechanism of high-energy (p,pn) reactions. It should be pointed out, however, that shell broadening may be sufficiently great in such a deeply buried shell to wash out the effect in question.

The present study concerns the experimental investigation of the occurrence of such discontinuities in the variation of (p,pn) cross section with neutron number for nuclei having 36–46 neutrons. Cross sections at 2.9 GeV are reported for Cu^{65}, Zn^{66}, Ge^{70}, Ge^{72}, Se^{76}, Br^{79}, and Br^{81}. Recently, measurements of the (p,pn) cross sections at 2.9 GeV for Ga^{69},[8] Ga^{71},[8] and As^{75},[9] have been performed in this laboratory. The results of all the above measurements are analyzed with the aid of Benioff's formalism[6] in the light of the above discussion.

II. EXPERIMENTAL PROCEDURE

A. Irradiations

The irradiations were performed in the circulating beam of the Cosmotron at an energy of 2.9 GeV. The target assembly was in a stationary position throughout

* Research performed under the auspices of the U. S. Atomic Energy Commission.
[1] H. Tyrén, P. Hillman, and Th. A. J. Maris, Nucl. Phys. **7**, 10 (1958).
[2] Th. A. J. Maris, P. Hillman, and H. Tyrén, Nucl. Phys. **7**, 1 (1958).
[3] T. J. Gooding and H. G. Pugh, Nucl. Phys. **18**, 46 (1960); J. P. Garron, J. C. Jacmart, M. Riou, C. Ruhla, J. Teillac, C. Caverzasio, and K. Strauch, Phys. Rev. Letters **7**, 261 (1961); G. Tibell, O. Sundberg, and U. Miklavzic, Phys. Letters **1**, 172 (1962).
[4] K. J. Foley, G. L. Salmon, and A. B. Clegg, Nucl. Phys. **31**, 43 (1962).
[5] K. J. Foley, A. B. Clegg, and G. L. Salmon, Nucl. Phys. **37**, 23 (1962).
[6] P. A. Benioff, Phys. Rev. **119**, 324 (1960).
[7] J. R. Grover (unpublished).
[8] N. T. Porile, Phys. Rev. **125**, 1379 (1962).
[9] S. Kaufman, Phys. Rev. **126**, 1189 (1962).

the run and was protected from low-energy spill-out protons by a retractable aluminum shutter. The number of protons striking the target was determined from the Na^{24} disintegration rate in an aluminum foil that was included for this purpose in the target stack. The cross section for the $Al^{27}(p,3pn)$ reaction was taken as 9.1 mb at 2.9 GeV.[10] The irradiation times ranged from 2 min to 3h. In the course of this study 31 separate Cosmotron irradiations were performed.

B. Targets

The targets consisted in most cases of enriched isotopes. Targets were prepared from the enriched material by either electrodeposition or sedimentation. Targets of Zn^{66} were thus prepared by electroplating zinc to a thickness of 2–3 mg/cm² onto 0.0001-in.-thick nickel foil. The germanium targets were prepared by electrodeposition of Cu_3Ge to a thickness of 5 mg/cm² onto 0.0001-in.-thick copper foil.[11] The selenium and bromine targets were prepared by sedimentation of elemental selenium and NH_4Br, respectively. The material was ground to a fine consistency, slurried with water or acetone, and filtered onto a carefully leveled disk of Whatman No. 41 filter paper. A thin layer of Duco cement was deposited on top of the target material by allowing a solution of Duco in acetone to evaporate to dryness. The sedimented targets had a thickness of 2–4 mg/cm² and had good adherence. In the case of copper, targets were prepared from 0.00025-in.-thick natural copper foil. The information on isotopic abundances and target composition is summarized in Table I.

The uniformity of the targets was checked visually and targets that appeared to be nonuniform were discarded. The uniformity of several targets was checked by x-ray fluorescence measurements using a Norelco X-ray Diffractometer. It has been found[12] that, for the mass region under consideration, the intensity of the fluorescent x rays is proportional to sample thickness for samples up to about 5 mg/cm² thick. It was found, in this fashion, that the nonuniformity of visually acceptable samples was less than 15%. The error introduced by such variations in sample thickness is of minor importance because, except for the intensity dropoff at the leading edge, the radial variation of the beam intensity is small for thin targets.[8]

In addition to the targets listed in Table I, targets of nickel, copper, and filter paper were irradiated in order to determine the contribution of the backing material to the observed activities. In no instance was a correction of more than 0.5% required. A bombardment of natural selenium was performed in order to obtain an estimate of the contribution of the other selenium isotopes (present in 9% abundance) to the activity of Se^{75}. In the cases of Ge^{70} and Br^{79}, the bombardments of Ge^{72} and Br^{81}, respectively, provided the necessary information for correction of the results. All the other targets were of sufficient isotopic purity to permit the determination of the (p,pn) cross section with an uncertainty of less than 2% from this source. In all these cases, the systematics of (p,pxn) cross sections[8] were used to estimate the contribution of other target isotopes. Several bombardments were performed for the bromine targets in which the cross section was determined as a function of target thickness. The purpose of these experiments was to check for the possible occurrence of hot-atom effects that might result in the loss of radiobromine from the target. The cross section was found to be independent of target thickness when the latter was varied by a factor of 5, provided that the target was at least 1 mg/cm² thick. While this experiment is suggestive, it does not conclusively prove the absence of hot-atom effects and this remains a possible source of error.

TABLE I. Isotopic abundance and composition of targets.

Target	Isotopic abundance	Composition
Cu^{65}	30.9%	Cu
Zn^{66} [a]	98.8%	Zn
Ge^{70} [a]	92.6%	Cu_3Ge
Ge^{72} [a]	96.4%	Cu_3Ge
Se^{76} [b]	91%	Se
Br^{79} [a]	95.1%	NH_4Br
Br^{81} [a,c]	96.3%	NH_4Br

[a] Obtained from Oak Rdge National Laboratory.
[b] Obtained from Atomic Energy Research Establishment, Harwell, England.
[c] The enrichment of Br^{81} was checked by neutron activation analysis. The ratio of Br^{82} and Br^{80} activities was obtained for an enriched Br^{81} sample and for natural bromine. The abundance of Br^{81} in the enriched sample was found to be 97.9 ±0.3% in fair agreement with the quoted value.

The target stack consisted of the target foil and of 3 aluminum foils on the downstream side of the target. The central aluminum foil, with a thickness of 2.5 or 7.0 mg/cm² was used to monitor the beam intensity. The other aluminum foils were used to compensate for recoil loss and to protect the monitor foil from recoils originating in the target foil. The target foil was oriented so that forward recoils were stopped in the backing foil. Recoils emitted at an angle of more than 90° to the beam were usually not collected, but the range of these recoils has been found[13,14] to be sufficiently small so that the error introduced by this procedure is negligible. After irradiation, the leading edge of the target stack was trimmed off and the foils were carefully cut from the target holder.

C. Chemical Procedures

The chemical purifications were in all cases based on standard radiochemical procedures.[15] Copper and zinc

[10] J. B. Cumming, J. Hudis, A. M. Poskanzer, and S. Kaufman, Phys. Rev., **128**, 2392 (1962).
[11] C. G. Fink and V. M. Dokras, Trans. Electrochem. Soc. **95**, 80 (1949).
[12] L. Remsberg (private communication).
[13] N. T. Porile (unpublished).
[14] E. R. Merz and A. A. Caretto, Phys. Rev. **126**, 1173 (1962).
[15] Subcommittee on Radiochemistry Monographs, NAS-NRC, 1961.

were purified by anion exchange separation, scavengings with $Fe(OH)_3$, and precipitation of CuCNS and ZnS, respectively. Germanium was separated by distillation of $GeCl_4$ in a stream of chlorine and precipitation of GeS_2. In some of the germanium bombardments arsenic was separated in order to determine the contribution of the $(p,2n)$ reaction. In this separation, germanium was distilled off, the arsenic product was allowed to decay to germanium, germanium carrier was added and germanium was redistilled. The chemical procedure for selenium consisted of a $GeCl_4$ distillation followed by a $SeBr_4$ distillation in a stream of HBr. Selenium was separated from arsenic by reduction to the metal with SO_2.

Bromine was purified by oxidation of the bromide to Br_2 with $KMnO_4$ and extraction into CCl_4. Bromine was back extracted as Br^- with aqueous $NaHSO_3$ and precipitated as AgBr. In view of the large number of oxidation states of bromine an experiment was performed to determine if the above procedure resulted in complete exchange between the active and inactive bromine atoms. Ammonium bromide was activated in the Brookhaven research reactor and bromine was separated according to the above procedure. The activity of this sample was compared with that of the aqueous residue from the CCl_4 extraction which should contain any nonextractable higher oxidation state species of bromine. An upper limit of 1% could be set on the latter on the basis of this experiment.

D. Radioactivity Measurements

A variety of detectors was used to determine the disintegration rate of the samples. In several instances a given sample was assayed with a number of different detectors as a check on the decay scheme and on the calibration procedures. The activity of nuclides decaying by positron emission was assayed by determination of the 0.51–0.51 MeV γ-ray coincidence rate with two 2-in.×2-in. NaI(Tl) detectors. The efficiency of this spectrometer was determined with a calibrated Na^{22} source. It was found that the counting rate was independent of positron energy provided that the source-to-detector distance was at least 5 in. when copper absorbers were used to annihilate the positrons.

The activity of positron or negatron emitters was also assayed with beta proportional counters. These counters had previously been calibrated by determination of the beta activity of a given nuclide with a 4π beta counter. The γ-ray emission rate of the samples was assayed with a scintillation spectrometer consisting of a 3-in. ×3-in. NaI(Tl) detector connected to either a 100-channel or a 256-channel pulse-height analyzer. The detector had previously been calibrated with a number of standard sources. This detector was also used for the determination of annihilation radiation resulting from positron emission. The analysis of γ-ray spectra was facilitated in a number of instances by the preparation of pure sources of a given nuclide. These sources were prepared by appropriate low-energy bombardments at the 60-in. cyclotron or by neutron activation in the reactor.

The disintegration rate of nuclides decaying by electron capture was determined by assay of the K x rays with an argon-methane proportional counter connected to a 100-channel pulse-height analyzer. The over-all efficiency of this detector was determined from careful geometry measurements and the known[16] efficiency of the counting gas for x rays. The detection methods employed for each nuclide as well as the pertinent decay scheme data[17,18] are summarized in Table II.

TABLE II. Radioactivity measurement procedures and assumed branching ratios.

Nuclide	Detector[a]	Branching ratio
12.9-h Cu^{64}	0.51–0.51	β^+—19%[b]
	Gamma	$\beta^+ + \beta^-$—58%[b]
	Beta	
245-day Zn^{65}	Gamma	1.11-MeV γ—49%[b]
40-h Ge^{69}	0.51–0.51	β^+—24%
	x ray	
11-day Ge^{71}	x ray	K capture—86%[c]
120-day Se^{75}	Gamma	0.26-MeV γ+0.28-MeV γ—85%; 0.40-MeV γ—11.6%[d]
	x ray	K capture—90%,[c] K conversion—8.3%[d]
6.5-min Br^{78}	Gamma	β^+—93%[b]
18-min Br^{80}	Gamma	0.62-MeV γ—13.8%[b]
	Beta	$\beta^- + \beta^+$—95%[b]
4.5-h Br^{80m}	Gamma	Radiations of Br^{80} detected
	Beta	

[a] The detectors are described in the text.
[b] From reference 17.
[c] Based on theoretical calculations for $\epsilon_K/\epsilon_{total}$.
[d] From reference 18.

In the course of this study the K/β^+ ratio for Ge^{69}, which was poorly known, was redetermined. A value of 2.85 was obtained on the basis of a determination of the positron and K x-ray disintegration rates of a Ge^{69} sample. This value assumes that the contribution of K x rays resulting from internal conversion processes is negligible.

III. RESULTS

The cross sections for the (p,pn) reactions obtained in this study are summarized in Table III. Several corrections had to be applied to the data to obtain these results. In a number of instances the product of the $(p,2n)$ reaction decays to the product of the (p,pn) reaction prior to separation. In order to correct the data for this effect the $(p,2n)$ cross sections were

[16] A. H. Compton and S. K. Allison, *X-Rays in Theory and Experiment* (D. Van Nostrand Co., New York, 1935).
[17] *Nuclear Data Sheets*, compiled by K. Way *et al.* (Printing and Publishing Office, National Academy of Sciences—National Research Council, Washington 25, D. C., 1960), NRC 59-2-13, 59-2-23, 59-5-47, and 59-1-52.
[18] W. F. Edwards and C. J. Gallagher, Nucl. Phys. **26**, 649 (1961).

TABLE III. Experimental cross sections for (p,pn) and $(p,2n)$ reactions at 2.9 GeV.

Target	(p,pn) cross section (mb)	
Cu^{65}	49±4	(3)[a]
Zn^{66}	50±2	(3)
Ge^{70}	59±3	(3)
Ge^{72}	70±4	(3)
Se^{76}	49±4	(3)
Br^{79}	56±3	(3)
$Br^{81} \rightarrow Br^{80m}$	31.5±3.4	(3)
$Br^{81} \rightarrow Br^{80g}$	27.7±3.0	(3)
Ga^{69}	58±6[b]	
Ga^{71}	59±4[b]	
As^{75}	46±4[c]	
	$(p,2n)$ cross section (mb)	
Ge^{70}	0.5	(1)
Ge^{72}	0.7	(1)

[a] The numbers in parenthesis refer to the number of separate determinations.
[b] From reference 8.
[c] From reference 9.

measured for Ge^{70} and Ge^{72} and the resulting values are listed in Table III. A cross section of 0.6 mb has also been recently reported[8] for the $Ga^{69}(p,2n)$ reaction at 2.9 GeV. The (p,pn) cross sections for Zn^{65} and Se^{76} were corrected for the contribution of the $(p,2n)$ reaction assuming the cross section for the latter was 0.6 mb while the cross sections for the germanium nuclides were corrected by use of the measured values. The corrections applied to the data to account for the contribution of minor isotopic constituents of the enriched targets have been described in Sec. IIb.

The errors listed in Table III are standard deviations from the mean value and also include an estimate of the systematic error ascribable to decay scheme or counting efficiency uncertainties. This error is in some cases based on the agreement between cross sections obtained on the basis of the different counting techniques listed in Table II. The cross sections obtained for Br^{81} based on the detection of the 0.62-MeV γ ray were almost a factor of two lower than those obtained on the basis of beta detection. We believe that this difference reflects an error in the branching ratio for the 0.62-MeV γ ray. The listed cross sections for Br^{81} are accordingly based only on the beta assay results.

In addition to the present results, (p,pn) cross sections have recently been determined for Ga^{69},[8] Ga^{71},[8] and As^{75},[9] at 2.9 GeV. The respective cross sections for these reactions, adjusted to the same value of the monitor cross section, are also listed in Table III. The cross sections for (p,pn) reactions in the mass region of interest thus appear to range from about 45 to 70 mb and exhibit the following trend with increasing neutron number. The cross sections increase from about 50 mb for $N=36$ to 60–70 mb for $N=40$, then fall below 50 mb at $N=42$, and finally increase again to about 60 mb at $N=46$. While the magnitude of this variation is not very large in view of the 5–10% uncertainties in the measurements it is given added weight by the generally good agreement in cross section between different targets having the same neutron number. The significance of this trend is discussed in the following section.

The $Cu^{65}(p,pn)$ cross section in the low GeV region has been determined by a number of investigators. Barr[19] quotes a value of 59 mb at 5.7 GeV, Markowitz *et al.*[20] obtained 55 mb at 2.2 GeV, and Hudis *et al.*[21] obtained 51 mb at 3 GeV. All these cross sections have been adjusted to conform with the monitor cross sections of Cumming *et al.*[10] It is seen that the present value is in good agreement with the recent value of Hudis *et al.*[21] To our knowledge, none of the other (p,pn) cross sections reported here have previously been measured in the low GeV region.

IV. DISCUSSION

The experimental (p,pn) cross sections may be compared with values calculated by use of Benioff's formalism.[6] The calculated cross sections at 3 GeV are given by the expression

$$\sigma = 36 \sum_{\substack{\text{allowed} \\ \text{shells}}} nM \text{ (mb)},$$

where n is the number of neutrons in a given shell and M is their fractional availability for the (p,pn) reaction. The numerical factor is related to the elementary particle scattering cross sections. The summation is carried out over all allowed shells, i.e., all shells for which the residual nucleus is formed in a particle-stable state. In order to evaluate the (p,pn) cross section, information is thus required on the energy levels of neutrons in the potential well of the nucleus. Several calculations of energy levels have been performed. Ross, Mark, and Lawson[22] calculated nucleon binding energies for a diffuse nuclear potential on the basis of the independent-particle model. Their results are only available, however, for closed-shell nuclides. Green[23] performed a similar calculation for all mass numbers but his treatment does not include spin-orbit coupling. Nilsson[24] has calculated nucleon binding energies as a function of nuclear deformation for the entire range of mass numbers. We have constructed a diagram of neutron energy levels on the basis of Nilsson's calculation for spherically shaped nuclei, adjusted to match the results of Ross, Mark, and Lawson[22] at closed neutron

[19] D. W. Barr, University of California Lawrence Radiation Laboratory Report UCRL-3793, 1957 (unpublished).
[20] S. S. Markowitz, F. S. Rowland, and G. Friedlander, Phys. Rev. **112**, 1295 (1958).
[21] J. Hudis, I. Dostrovsky, G. Friedlander, J. R. Grover, N. T. Porile, L. P. Remsberg, R. W. Stoenner, and S. Tanaka, Phys. Rev. **129**, 434 (1963).
[22] A. A. Ross, H. Mark, and R. D. Lawson, Phys. Rev. **102**, 1613 (1956).
[23] A. E. S. Green, Phys. Rev. **102**, 1325 (1956).
[24] S. G. Nilsson, Kgl. Danske Videnskab. Selskab, Mat. Fys. Medd. **29**, 16 (1955).

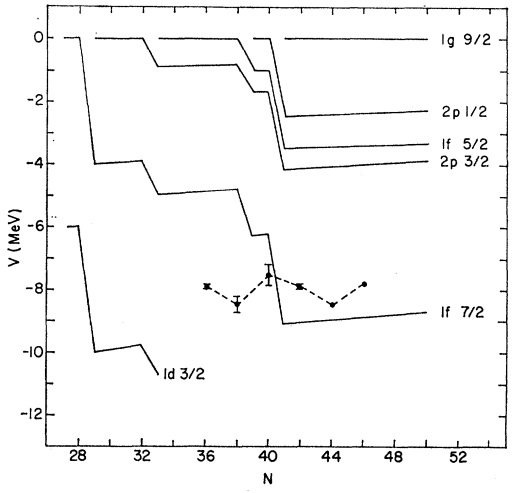

FIG. 1. Neutron energy levels in the region of 28–50 neutrons. The energy of a given level is expressed relative to that of the topmost level. The dashed line gives the neutron separation energy for the nuclides of interest.

shells. Adjustments of up to 2 MeV in the relative energy of the various shells were necessary, indicating the uncertainty in such a calculation. The calculation also does not include the effect of nucleon pairing although all the (p,pn) reactions considered here involve the breaking of a neutron pair. The uppermost neutron levels for the region of $N=28$–50 are shown in Fig. 1. The energies of these levels are given relative to the energy of the top neutron level. The dashed line in Fig. 1 connects the neutron separation energies of the product nuclei resulting from the (p,pn) reactions in question. The vertical flags indicate the range in separation energies of the products studied at each neutron number. It is seen that the separation energy line crosses the $1f_{7/2}$ shell between N=40 and $N=42$. To a first approximation this shell should become unavailable for the (p,pn) reaction at the neutron number corresponding to this crossing, leading in turn to a decrease in the (p,pn) cross section. In order to estimate the magnitude of this effect the (p,pn) cross section may be calculated for the neutron number range of interest on the assumption that the $1f_{7/2}$ shell either is or is not available. The results of such a calculation are given by the two solid lines in Fig. 2. The cross sections were obtained for all even neutron numbers between 34 and 46 by use of the fractional availability coefficients, M, given by Benioff. The calculation was performed with a value for r_0, the half-density radius parameter, of 1.07 F.[25] It is seen that the expected contribution of the $1f_{7/2}$ shell for $N=40$–42 is about 20 mb.

The experimental (p,pn) cross sections are compared with the calculated values in Fig. 2. Good agreement is obtained on the assumption that the $1f_{7/2}$ shell is available up to $N=40$ and unavailable thereafter.

[25] R. Hofstadter, Ann. Rev. Nucl. Sci. 7, 231 (1957).

This agreement, if taken at face value, would be confirmatory evidence for the correct position of the $1f_{7/2}$ shell as given in Fig. 1. Before this conclusion can be drawn the statistical significance of the results must be examined and the effect of a number of complicating factors must be considered.

A statistical analysis of the data may be performed by a comparison of the fit of the calculated line to that obtained on the assumption that the variation of (p,pn) cross section with neutron number is linear. A least-squares fit to the data was performed for this purpose. The cross sections were weighted by the inverse of the respective variances. The results of the statistical analysis are presented in Table IV. The values of

TABLE IV. Statistical analysis of data for different models of (p,pn) cross sections.

Model	χ^2	F	Confidence level
Calculated curve	14.3	2.27	86%
Linear variation of σ with N	28.9		
Two straight lines	4.79	4.53	96%
One straight line	28.9		

$\chi^2=\sum_i \Delta_i^2/\sigma_i^2$ are computed for each of the assumed functions, where Δ_i is the deviation of a given point from the assumed functional value and σ_i is the experimental standard deviation of that point. The respective fits are compared by means of the F test, where $F=(\chi^2_{\text{linear}}/8)/(\chi^2_{\text{calc}}/9)$. The values of χ^2 are divided by the appropriate number of degrees of freedom in the determination of F. It is assumed that a single constraint is imposed on the fit to the calculated curve by the choice

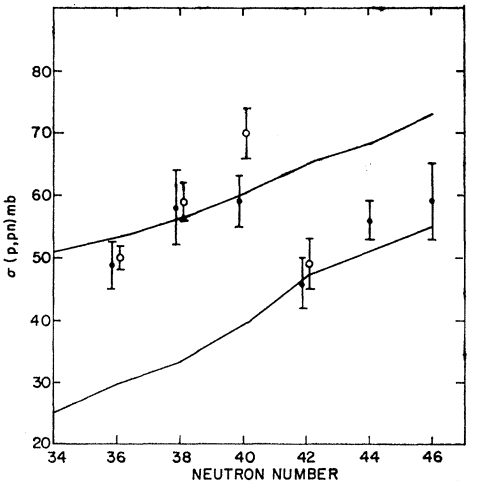

FIG. 2. Calculated and experimental (p,pn) cross sections. The calculation is based on reference 6 with $r_0=1.07$ F. Top line—$1f_{7/2}$ shell available; bottom line—$1f_{7/2}$ shell unavailable. Closed points—odd A target; open points—even A target.

of r_0. It is seen that the data are in better agreement with the calculated curve based on Benioff's treatment and the aforesaid assumptions about the availability of the $f_{7/2}$ shell at an 86% confidence level.

It is also of interest to determine if the decrease in (p,pn) cross section observed at $N=42$ is statistically significant without reference to the theoretical implications of this point. For this purpose the data were divided into two groups, one for $N=36$–40 and the other for $N=42$–46, and a least-squares fit to the weighted points in each group was performed. It was assumed that $\sigma(p,pn)$ varied linearly with N within each group. The resultant fit was compared with that obtained for a single straight line by the F test, where $F=(\chi^2_{\text{one line}}/8)/(\chi^2_{\text{two lines}}/6)$. The results are summarized in Table IV and it is seen that the two-line fit is superior at a 96% confidence level.

There are a number of factors that complicate the simple model of the (p,pn) reaction discussed so far. The position of the $1f_{7/2}$ shell has thus been compared with the neutron separation energy. In a number of cases, however, the proton separation energy is lower than the neutron separation energy, the maximum difference amounting to 2 MeV for Br^{78}. It is most unlikely, however, that the emission of 2 MeV protons will occur in view of the fact that the Coulomb barrier against proton emission is 7–8 MeV in this mass region. The same consideration applies to the evaporation of alpha particles. It is thus reasonable to assume that all states for which neutron emission is energetically impossible are stable to particle emission and de-excite by gamma-ray emission.

It is also possible, of course, that states for which neutron emission is energetically possible will still lead to the (p,pn) rather than the $(p,p2n)$ product because of preferential de-excitation by gamma-ray emission. The latter process can be of importance if the centrifugal barrier against neutron emission is large. This situation will occur if the excited states populated in the (p,pn) reaction have spin values that are very different from those of the states available following subsequent neutron evaporation. This situation has been considered by Grover.[26] He points out that the effect of γ-ray emission depends in a detailed way on the particular nuclide under consideration and that cases where γ-ray emission is still important at $\geqslant 0.5$ MeV above the neutron separation energy are not uncommon. A detailed analysis of the mass region under consideration awaits more information about the excited states of the nuclides in question. It is clear, however, that γ-ray competition may affect the previous discussion concerning the position of the $f_{7/2}$ shell relative to the neutron separation energy line in the region of the crossing. It may thus be possible that the $1f_{7/2}$ shell has already fallen below the separation energy line at $N=40$, but is still available because of γ-ray competition.

An effect that works in the opposite direction from γ-ray competition is the occurrence of nuclear rearrangement following the prompt knock-out of a target neutron. The magnitude of the rearrangement energy and its effect on (p,pn) cross sections has been considered by Benioff.[6,27] While the energy release appears to be small when compared to the neutron separation energy, it may still be comparable to the energy for which γ-ray de-excitation competes with neutron emission. If this is so, then the two effects will tend to cancel each other as far as the energy at which the $1f_{7/2}$ shell becomes unavailable is concerned.

This discussion has so far assumed that neutrons lying deep in the nuclear potential well may be associated with a single configuration occurring at a unique energy. In fact, configuration mixing is well known to occur in the region between closed shells. As a result the ground-state configuration of the target nucleus can have a number of parent states distributed over a range of excitation energies. The resulting broadening of the excitation energy spectrum following the knock-out of a neutron will tend to smear out the effect under consideration. Energy broadening may also occur because of the very short lifetime of the "hole" state formed by the knock-out of a deeply buried neutron. Further, the possible occurrence of nuclear deformation in the region between closed shells will lead to a splitting of the independent particle levels and will thus also result in energy broadening. The occurrence of multiple-scattering processes involving the incident and emitted particles will also result in a spectrum of residual excitation energies.

In general it is rather difficult to evaluate the effect of these various factors on the occurrence of a sharp discontinuity in the availability of the $1f_{7/2}$ shell. Perhaps the experimental results presented here, and their agreement with a simple calculation in which these effects are neglected, can be taken as evidence that the latter are relatively small. We now proceed to show that this is indeed the case for the effect associated with the splitting of levels due to the occurrence of nuclear deformation.

The occurrence of nuclear deformation may be determined from a calculation of the total binding energy of a nucleus as a function of nuclear deformation. The ground-state configuration is then assumed to have the shape for which the total energy is a minimum. The calculation may be performed by use of the single-particle energies given by Nilsson,[24] which may be summed to obtain the total energy. The results may be expressed as the difference between the total binding energy of the nucleus for the spherical case and for the deformed case, for several values of the deformation parameter, δ.[24] Table V shows the results of the calculation for the nuclides of interest in this study. The calculation assumes identical binding

[26] J. R. Grover, Phys. Rev. **123**, 267 (1961).

[27] P. A. Benioff, Nucl. Phys. **26**, 68 (1961).

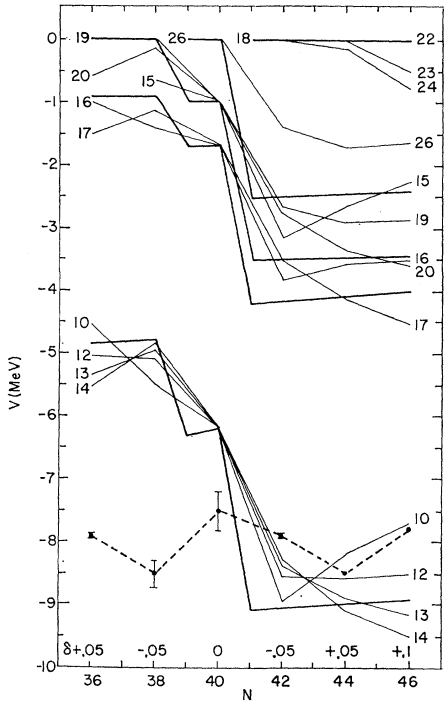

FIG. 3. Neutron energy levels in the region 36–46 neutrons for a deformed potential. The values of the deformation parameter δ at each even neutron number are listed along the abscissa. The levels are identified by their Nilsson numbers. The heavy line gives the energy levels for a spherical nucleus and is taken from Fig. 1. The dashed line gives the neutron separation energy for the nuclides of interest.

energies for proton and neutron states and use is made of the eigenvalues listed in Table I of reference 24. It is seen that a prolate configuration is favored for Zn^{66} and Br^{81}, while an oblate configuration is favored for Ge^{70}, As^{75}, and Br^{79}. As a result of this deformation a level of half-integral angular momentum j splits into $(j+\frac{1}{2})$ Nilsson levels. The energy of these levels in the nuclear potential may be determined from the eigenstate values listed by Nilsson.[24] The position of the levels corresponding to the undeformed single-particle levels in Fig. 1 is shown in Fig. 3. For simplicity the levels are given for an average value of δ at each even neutron number. The values of δ are listed along the abscissa and the levels are identified by their Nilsson numbers. The position of the undeformed levels, given in Fig. 1, is shown by the heavy lines in Fig. 3. The position of the Nilsson levels in the nuclear potential well has been adjusted so that the energy difference between the corresponding levels for the deformed and spherical cases is the same in Fig. 3 as it is in Nilsson's calculation.[24] The dashed line in Fig. 3 once again refers to the neutron separation energy.

TABLE V. Effect of deformation on total nuclear binding energy. The difference in energy between a spherical and a deformed configuration is given for several values of the deformation parameter δ.

	ΔE (MeV)				
Nucleus	$\delta=-0.2$	$\delta=-0.1$	$\delta=0.0$	$\delta=0.1$	$\delta=0.2$
Cu^{65}	5.00	0.37	0.00	0.28	3.64
Zn^{66}	3.75	0.04	0.00	−0.32	5.45
Ga^{69}	5.92	0.17	0.00	0.74	1.88
Ge^{70}	5.66	−0.37	0.00	0.27	1.07
Ga^{71}	2.24	2.02	0.00	1.74	5.15
Ge^{72}	2.00	1.48	0.00	1.28	4.34
As^{75}	1.38	−0.08	0.00	0.05	1.66
Se^{76}	1.51	0.15	0.00	0.33	1.23
Br^{79}	2.84	−0.12	0.00	−0.09	2.28
Br^{81}	7.51	0.18	0.00	−0.36	1.88

The occurrence of deformation appears to have only a slight effect on the availability of levels for the (p,pn) reaction due largely to the fact that the deformation in this mass region is small. The only difference is that the 2 neutrons in level No. 10 now appear to be available for the (p,pn) reaction in Br^{79} and Br^{81}, whereas they were unavailable in the case of no deformation. The calculated cross sections for these two nuclides should thus be slightly larger than indicated in Fig. 2, leading to somewhat better over-all agreement with the experimental results.

The (p,pn) reaction on Br^{81} leads to the formation of $Br^{80g}(1+)$ and $Br^{80m}(5-)$. The isomer ratio may be compared with a value calculated on the basis of Benioff's fractional availability coefficients on the assumption that the $1g_{9/2}$, $2p_{1/2}$, $1f_{5/2}$, and $2p_{3/2}$ neutron shells contribute to the reaction. The removal of a neutron in one of the above shells from $Br^{81}(3/2-)$ leads to a set of states having angular momentum values j_e ranging from $|j_1-\frac{3}{2}|$ to $|j_1+\frac{3}{2}|$ and relative populations varying as $(2je+1)$, where j_1 is the angular momentum of the neutron in question. The de-excitation of these states to either the ground or isomeric state proceeds by a cascade of γ rays. This part of the problem may be treated in the manner of Huizenga and Vandenbosch.[28] We assume that the γ-ray cascade consists of dipole radiation and that the relative probability for obtaining a state with spin J_f from the decay of a state with spin J is given by the spin-dependent part of the level density, $P(J_f)=(2J_f+1)\times\exp[-(J_f+\frac{1}{2})^2/2\sigma^2]$. The average number of γ rays emitted/cascade has been found to be 3–4 in the case of (n,γ) reactions.[29] The residual nuclei following (p,pn) cascades have lower excitation energies than the (n,γ) reaction products so that it is reasonable to assume that the γ-ray multiplicity will be lower. We have, somewhat arbitrarily, assumed a multiplicity of 2 for the cascade following knock-out of a $g_{9/2}$ or a $p_{1/2}$ neutron, and one of 3 for that following removal of an $f_{5/2}$ or $p_{3/2}$ neutron. The calculation has been performed for $\sigma=4$ and it is further assumed that the

[28] J. R. Huizenga and R. Vandenbosch, Phys. Rev. **120**, 1305 (1960).

[29] L. V. Groshev, A. M. Demidov, V. N. Lutsenko, and V. I. Pelekhov, *Proceedings of the Second United Nations International Conference on the Peaceful Uses of Atomic Energy, Geneva, September, 1958* (United Nations, Geneva, 1958), Vol. 15, Paper P/2029.

TABLE VI. Calculation of $Br^{81}(p,pn)$ isomer ratio.

Neutron shell	Spins of product states	Relative weight	No. of γ	Isomeric state branch	Rel. wt. ×isomer branch	No. of neutrons n	M	$(\Sigma m)\times nM$	$(\Sigma g)\times nM$
$1g_{9/2}$	3	0.175	2	0.52	0.091	6	0.123	0.648	0.090
	4	0.225	2	0.83	0.187				
	5	0.275	2	1.0	0.275				
	6	0.325	2	1.0	0.325				
					$\Sigma m=0.878$				
$2p_{1/2}$	1	0.375	2	0	0	2	0.113	0.028	0.198
	2	0.625	2	0.20	0.125				
					$\Sigma m=0.125$				
$1f_{5/2}$	1	0.125	3	0.11	0.014	6	0.075	0.234	0.216
	2	0.208	3	0.29	0.060				
	3	0.292	3	0.53	0.155				
	4	0.375	3	0.78	0.292				
					$\Sigma m=0.521$				
$2p_{3/2}$	0	0.063	3	0	0	4	0.113	0.155	0.296
	1	0.187	3	0.11	0.021				
	2	0.313	3	0.29	0.091				
	3	0.437	3	0.53	0.232				
					$\Sigma m=0.344$				
								1.065	0.800
								$\sigma_m/\sigma_g=1.33$	

last emitted γ ray leads to either the ground or isomeric state depending on which transition involves a smaller spin change.

The calculation is outlined in Table VI. The contribution of each of the neutron shells to the ground and isomeric states is determined, and weighted by the number of neutrons in each shell and by their fractional availability. The isomer ratio is obtained from the sum of the weighted contributions and is 1.33. This value may be compared with the experimental value of 1.14 ± 0.17. The calculated result depends, of course, on the assumptions about the γ-ray multiplicity. If the latter is taken as 1 for all shells, the calculated ratio becomes 1.17. The isomer ratio may also be calculated on the assumption that the filled $f_{7/2}$ shell contributes to the (p,pn) reaction. A value of 1.52 is obtained on the assumption that 3 γ rays are emitted in the de-excitation of the states resulting from the knock-out of an $f_{7/2}$ neutron. While the calculated isomer ratio thus is less sensitive than the calculated (p,pn) cross section to the availability of the $f_{7/2}$ shell, it does provide confirmatory evidence for the conclusions based on the latter results.

In summary, the cross-section and isomer ratio results presented in this study appear to bear out the relation between (p,pn) cross sections and the position of neutron shells in the potential well of the nucleus. While the effect associated with the sudden unavailability of the $1f_{7/2}$ shell is not much larger than the uncertainty in experimental cross sections, it does appear to be statistically significant. The effect of nuclear deformation on the availability of neutron levels has been considered and found to be small in the mass region under consideration.

ACKNOWLEDGMENTS

The authors wish to thank R. W. Stoenner and J. K. Rowley for the chemical yield analyses, R. Withnell for help with target preparation, and the operating crew of the Cosmotron for their cooperation. The authors also wish to thank a number of their colleagues for valuable discussions and J. R. Grover for a critical reading of the manuscript.